Metabolomic profiling on plasma reveals potential biomarkers for screening and early diagnosis of intestinal-type gastric cancer and precancerous stages

Lijing Du
School of Pharmacy, Shanghai Jiao Tong University
Shasha Li
The Second Clinical College of Guangzhou University of Chinese Medicine
Xue Xiao
Guangdong Pharmaceutical University
Jin Li
The 903rd Hospital of PLA
Huizi Jin
Shanghai Jiao Tong University
Zhaolai Hua
People's Hospital of Yangzhong City
Juming Ma
The 903rd Hospital of PLA
Xi Wang
The 903rd Hospital of PLA
Shikai Yan (shkyan@sjtu.edu.cn)
Shanghai Jiao Tong University of pharmacy

Research article

Keywords: Intestinal-type gastric cancer, Metabolomics, Biomarkers, Pathway analysis, UPLC-Q-TOF/MS

Posted Date: November 12th, 2020

DOI: https://doi.org/10.21203/rs.3.rs-18127/v3

Abstract

Background: Gastric cancer (GC) with majority of intestinal-type adenocaricinoma remains one of the most common cancers all over the world. GC faces a great challenge in the clinical diagnosis, that it often can be detected at advanced stages, and leads to the loss of optimum time for treatment and poor prognosis. Thus, there is a critical need to develop effective and noninvasive strategies for early diagnosis of the disease process.

Methods: Totally, 82 participants were enrolled in the study, including 50 chronic superficial gastritis (CSG) patients, 7 intestinal-type early gastric cancer (EGC) and 25 intestinal-type advanced gastric cancer (AGC) ones. Metabolites profiling on patient plasma was performed using ultra-high performance liquid chromatography coupled with quadrupole-time-of-flight mass spectrometry (UPLC-Q-TOF/MS). Principal components analysis, orthogonal partial least squares-discriminant analysis as well as Random Forest were utilized to evaluate the variation on endogenous metabolites for intestinal-type GC patients and to screen potential biomarkers. Furthermore, the proposed biomarkers were used to create logistic regression models, which discrimination efficiency and accuracy was ascertained by receiver operating characteristic curve (ROC) analysis. Metabolic pathway analysis was carried out on MetaboAnalyst.

Results: Totally 50 metabolites were detected with differentially expression among CSG, intestinal-type EGC and AGC patients. L-carnitine, L-proline, pyruvaldehyde, phosphatidylcholines (PC) (14:0/18:0), lysophosphatidylcholine (14:0) (LysoPC 14:0), lysinoalanine were defined as the potential biomarker panel for the diagnosis among CSG and EGC patients. Compared with EGC patients, 6 significantly changed metabolites, PC(O-18:0/0:0) and LysoPC(20:4(5Z,8Z,11Z,14Z)) were found to be up-regulated in AGC patients, whereas L-proline, L-valine, adrenic acid and pyruvaldehyde down-regulated. ROC analysis demonstrated a high diagnostic performance for metabolite panels with area under the curve (AUC) of 0.931 to 1. Moreover, the metabolomic pathway analysis revealed several metabolism pathway disorders, including amino acid and lipid metabolisms, in intestinal-type GC patients.

Conclusions: In this study, a total of six metabolites were identified to contribute significantly to the diagnosis of intestinal-type GC and precancerous stages, respectively, and over 93.1% AUC value was achieved in AUC test on biomarker panels. It indicated that the biomarker panels are sensitive to the early diagnosis of intestinal-type GC disease, which is expected to be developed as a promising diagnostic and prognostic tool for disease stratification studies.

Background

The International Agency for Research on Cancer estimates that gastric cancer (GC) is the fifth most prevalent malignancy and the third mortality of cancer death all over the world [1]. GC presents in two major distinct morphological subtypes, intestinal and diffuse-type gastric cancers. The intestinal-type GC predominates in high risk geographic areas, such as China, and its incidence increases with age. To date, surgery is the most preferred treatment, but five year survival rate is often poor. [2, 3]. Generally accepted, human gastric carcinogenesis initiated by normal mucosa, followed by chronic superficial gastritis (CSG), then chronic atrophic gastritis, to intestinal metaplasia, and finally by dysplasia and gastric cancer [4]. Therefore, early prevention on gastric precancerous lesions and diseases could reduce the incidence of GC. In recent decades, diagnostic methods based on endoscopic examination, pathological section and barium meal examination have been widely applied to GC patients [5]. However, these screening methods are limited by various disadvantages, as they are time-consuming, involve a high level of invasiveness, and are laborious and potentially harmful to patients. Thus, establishment of a sensitive, noninvasive examination method for early detection and prognosis prediction in GC patients is of significant importance.

Metabolomics is an emerging science involving the profiling changes in small-molecular metabolites produced by a biological system under certain conditions [6]. It seems to be a very promising method for biomarker discovery due to the dynamic responses of the metabolome that reflects upstream biological processes in the body. It has several major advantages, such as the readily availability, noninvasive and high sensitivity [7]. For the past few years, metabolomics has been utilized for analysis of metabolic alterations caused by cancers and other diseases, which has led to substantial advances in the discovery of biomarkers and early diagnosis [8].

Biomarkers are small-molecular intermediates and end products of active cellular processes, forming a correlation between molecular metabolic changes and phenotype [9, 10]. Therefore, they reflect alterations of the physiological state of a biological system (cell, tissue or organism) at a certain point in time. There is no doubt that one of the greatest challenges for biomarker-related is discovering biomarkers that accurately distinguish cancer from precancerous stages, where overlapping signs and symptoms (unintentional weight loss or vague epigastric pain) make differential clinical diagnosis difficult [11]. Till now, few studies on metabolic changes for screening and early diagnosis of intestinal-type GC and precancerous stages have been applied in clinical practice, which are needed to be further explored.

In this work, we developed an ultra-high performance liquid chromatography coupled with quadrupole-time-of-flight mass spectrometry (UPLC-Q-TOF/MS) and metabolomics profiling approach for determining intestinal-type GC staging and precancerous (CSG). Briefly, multivariate analyses were utilized to identify differential metabolites that related to intestinal-type GC staging and CSG groups. On the basis of potential biomarkers, the related metabolic pathways and correlation networks were investigated and the global metabolic features were discussed.

Methods

Patient information and sample collection

The present study was approved by the ethics Committee of the People's Hospital of Yangzhong City (Yangzhong, China) and all participants provided written informed consent. A total of 86 individual patients, who had CSG and intestinal-type GC were recruited at the People's Hospital of Yangzhong City between July and December, 2015. All of tissue specimens were examined by gastroscopic biopsy or pathological examination after surgery. According to the results from pathologic diagnosis, the 86 samples were divided into three groups, including fifty cases of CSG (mean age ± SD, 52.1 ± 7.0 years), seven cases of intestinal-type EGC (mean age ± SD, 66.3 ± 11.9 years) and twenty-five cases of intestinal-type advanced gastric cancer (AGC, mean age ± SD, 67.0 ± 9.7 years). Among them, four cases of patients who had a history of chemotherapy or surgical treatment were excluded from this study. Atrophic gastritis was rare in the real world of Yangzhong City, a well-known high-risk area of gastric cancers in China where our specimens were collected. Thus, we did not enroll cases with atrophic gastritis in the present study [12]. Details of basic information of patients with CSG and intestinal-type GC staging are shown in Table S1.

5 mL venous blood samples from all patients were collected under fasting conditions and added in heparin sodium anti-coagulated tube. The collected whole blood was refrigerated at 4 ℃ within 15 min and centrifuged at 2000 rpm for 15 min within 4 h. Plasma was carefully transferred to an Eppendorf tube, and stored at -80 ℃ until use.

Chemicals and reagents

Acetonitrile, methanol, formic acid and isopropanol were purchased from J. T. Baker Chemical Co. (Phillipsburg, New Jersey, USA). All chemical reagents were HPLC grade. Purified water was produced by a Milli-Q Reagent Water System (Millipore, MA, USA).

Sample preparation

All frozen plasma samples were thawed completely at room temperature for 3 h. Then, 100 μL plasma samples were transferred to Eppendorf tubes, and 300 μL methanol/acetonitrile solution (v/v, 1:1) containing 2-Chloro-L-phenylalanine (5 μg/mL) as internal standard was added. Mixed sample was vortex-mixed for 30 s and placed at 4 °C for 1 h. Vortex-mix again for 30s and kept at 4°C for 3 h to fully precipitate the protein in the plasma. Finally, the mixture was centrifuged at 15000 rpm for 10 min at 4˚C, and the clear supernatant was collected to injection vial for UPLC-Q-TOF/MS analysis.

UPLC-Q-TOF/MS analysis

The metabolomic analysis was carried out on an ACQUITY UPLC (Waters) system equipped with Micromass quadrupole-time-of-flight mass spectrometer (Q-TOF/MS) (Waters Corp., Milford, USA). Plasma metabolites were separated on a Acquity BEH-C18 column (100 mm × 2.1 mm i.d., 1.7 μm; Waters, Milford, USA) with the column oven temperature maintained at 50 °C.

Mobile phase A consisted of 0.1% formic acid in water and mobile phase B used the mixture of B-isopropanol, acetonitrile, methanol, formic acid (20: 40: 40: 0.1 (v/v)). The gradient program (A/B, v/v) was changed from 98/2 to 0/100 for 12.5 min with a constant flow rate of 0.4 mL/min. Injection volume was set at 3 μL. MS parameters were as follows: mode, positive ion; capillary voltage, 3000 V; cone voltage, 35 V; collision energy, 3 eV; ion source temperature, 115 °C; desolvent gas temperature, 350 °C; desolvent gas flow, 600 L/h; full scan range, 50-1000 m/z. The mass spectrometric data were recorded with a scan time of 0.3 s and an inter-scan delay of 0.02 s. To evaluate data quality and reliability, a quality control (QC) sample was injected and analyzed once every 10 study samples.

Statistical analysis

The data collected from MS were processed using Progenesis QI, and then analyzed by SPSS 18.0. Statistical significance differences were established at $P < 0.05$. Data following a normal distribution were subjected to Student's t-test. Non-parametric Mann–Whitney test was used when normality assumption was violated. All statistical analysis and subsequent graphics generations were performed using GraphPad Prism version 8.0 (GraphPad Software, USA). Then, multivariate analysis and modeling were performed by SIMCA-P software (14.0, Umetrics AB), including principal component analysis (PCA) and orthogonal partial least squares-discriminant analysis (OPLS-DA). Random Forest curves were plotted by one-step metabolomics (One-MAP) platform (http://www.5omics.com/). The dataset was randomly divided into the discovery set (2/3 of samples) and the validation set (1/3 samples), and the tree number was set as 500. A fixed random state was used in all calculations to ensure that the model predictions were reproducible. Out-of-bag (OOB) error was used as cross-validation step in the evaluation of the prediction error. Significantly metabolites between two groups were identified by variable importance in the projection (VIP)□1 and $P < 0.05$. Finally, the structure information of differentially expressed metabolites was further identified based on MS^2 fragments and database of HMDB, METLIN, LIPID, SERUM and KEGG, etc. SPSS was used to draw receiver operating characteristic (ROC) curves to display the level and diagnosability of potential biomarkers directly and metabolome pathway maps were retrieved from online MetaboAnalyst 4.0 (https://www.metaboanalyst.ca/).

Results

Metabolites detection and identification

A full-scan detection of plasma metabolites was performed by UPLC-Q-TOF/MS, including 50 cases of CSG, 7 cases of intestinal-type EGC and 25 cases of intestinal-type AGC, which involved principal components that account for the majority of the differences in the data. In conjunction with the Progenesis QI package, UPLC-Q-TOF/MS analysis of plasma metabolites contained three typical total ion current (TIC) chromatograms, as shown in Fig. 1. A total of 2666 peaks were detected and 50 differential metabolites were authentically identified, including L-proline, L-isoleucine, L-leucine, L-valine, lysine alanine, lysophosphatidylcholines (LysoPC) (12), phosphatidylcholines (PC) (16), phosphatidylethanolamines (6), L-carnitine, creatine, cholesterol, cholic acid, tyramine, uric acid, capryl carnitine, pyruvaldehyde, docosatrienoic acid, malonaldehyde and 1-sphingosine phosphate, etc. The identity of metabolites based on the following criteria: VIP score > 1, P□0.05 in the EZinfo software, and metabolites match in the databases of HMDB, LIPID MAPS and SERUM.

Differential plasma metabolic profiles among groups

Metabolite differences in CSG and *intestinal-type* EGC

Using SIMcA-P software, PCA as an unsupervised method and OPLS-DA as a supervised method were performed to discriminate the overall metabolic profiles between CSG and intestinal-type EGC patients. The score plots of PCA and OPLS-DA are presented in Fig. 2A-B. Subjected to the inter-group PCA analysis, it was observed that there is no obvious clustering pattern between the two groups. OPLS-DA (CSG vs EGC) revealed a well gathering trend and complete separation in score plot. Of all peaks detected by UPLC-Q-TOF/MS, the peak areas of 30 peaks were statistically different between CSG and intestinal-type EGC patients (VIP□1, P□0.05), and these signals were identified by database of HMDB, LIPID MAPS and Serum. After that, the molecules responsible for these peaks were further identified by comparing the MS/MS spectra and Metlin database. Six metabolites, named L-carnitine, L-proline, pyruvaldehyde, PC(14:0/18:0), LysoPC(14:0) and lysinoalanine were definited in

metabolic profiles. Identification and statistic analysis indicated significant elevation of L-carnitine, L-proline, pyruvaldehyde, PC(14:0/18:0), LysoPC(14:0) and lysinoalanine were definited in metabolic profile, while revealing significant reduction of LysoPC(14:0) and lysinoalanine, in intestinal-type EGC compared with CSG, as shown in Table 1. Actual fold-change values were represented as scatter dot plots in Fig. S3.

Table 1 Statistically significant metabolites for comparison of CSG and intestinal-type EGC patients

NO	Retention time(min)	m/z	Compound	VIP value	P value	|log2 FC|	Means ± SEM	Confidence interval (95%)	The trend of EGC
1	0.67	162.11	L-Carnitine	1	0.0081*	0.50	3014 ± 882.5	(1246 to 4783)	↑
2	2.04	138.06	L-Proline	1	0.0003*	9.63	399.7 ± 85.42	(228.6 to 570.9)	↑
3	0.68	114.07	Pyruvaldehyde	1	0.0036	0.35	800.2 ± 263.2	(272.7 to 1328)	↑
4	10.30	734.57	PC(14:0/18:0)	1	<0.0001*	0.55	4044 ± 906.4	(2227 to 5860)	↑
5	5.65	468.31	LysoPC(14:0)	1	0.0081*	1.16	-1340 ± 558.0	(-2458 to -221.7)	↓
6	2.85	251.17	Lysinoalanine	1	0.002	2.24	-750.6 ± 421.5	(-1595 to 94.11)	↓

Parameters remaining significant after FDR correction are marked with a *

Metabolite differences in intestinal-type EGC and AGC

Similarly, a PCA analysis was used to explore the metabolic profiling differences between the intestinal-type EGC and AGC patients, and the results are presented in Fig. 2C. There were no distinctive differences between intestinal-type EGC and AGC groups. Then, the OPLS-DA model was launched (Fig. 2D). Based on the criteria of OPLS-DA (VIP > 1 and P < 0.05), 16 statistically differentially expressed metabolic molecules in total were screened out and finally 6 metabolic molecules were identified as potential metabolite biomarkers between the two groups. The significantly changed 6 metabolites listed in Table 2. PC(O-18:0/0:0) and LysoPC(20:4(5Z,8Z,11Z,14Z)) were found to be up-regulated, whereas L-proline, L-valine, adrenic acid and pyruvaldehyde to be down-regulated in intestinal-type AGC patients. Actual fold-change values were represented as scatter dot plots in Fig. S3.

Table 2 Statistically significant differences in metabolite levels between intestinal-type EGC and AGC groups

NO	Retention time(min)	m/z	Compound	VIP value	P value	|log2FC|	Means ± SEM	Confidence interval (95%)	The trend of EGC
1	2.04	138.06	L-Proline	1	0.0113*	0.53	2200 ± 977.3	204.4 to 4196	↓
2	0.73	118.08	L-Valine	1	0.0051*	0.36	2058 ± 936.6	144.8 to 3971	↓
3	4.31	355.26	Adrenic acid	1	0.0159*	8.73	425.5 ± 314.2	-216.2 to 1067	↓
4	7.96	551.43	PC(O-18:0/0:0)	1	0.0076*	0.52	-1497 ± 523.1	-2565 to -428.2	↑
5	5.91	544.34	LysoPC(20:4(5Z,8Z,11Z,14Z))	1	0.0153*	0.58	-2644 ± 1028	-4743 to -543.8	↑
6	0.68	114.06	Pyruvaldehyde	1	0.0352	0.30	954.0 ± 650.4	-374.2 to 2282	↓

Parameters remaining significant after FDR correction are marked with a *

Construction of Random Forest modelling

Random Forest, a supervised machine-learning algorithm, was used as a classifier capable of sorting CSG, EGC and AGC patients. As a classification result, ROC-curves were generated, which summarize all classification runs and estimate classification performance for all available data. As shown in Fig. 2E, the area under the receiver operating curve (AUC) was 97.65% (95% confidence interval [CI], 93.83–100%) in the testing set, suggesting that patients with CSG could be effectively distinguished from the EGC patients. Consistently, the AUC for distinguishing EGC from AGC was 60.94% (95% CI, 42.79–79.09%) in the testing set (Fig. 2F). The OOB error values were 0.123 and 0.219, respectively.

Discriminant models establishment based on the ROC analysis

ROC analysis is generally considered as a standard method for effectiveness assessment of diagnostic biomarkers. In this study, an in-depth ROC curve analysis was performed for 6 potential biomarkers (CSG vs EGC) and possible biomarker combinations. AUC represents the overall accuracy of intestinal-type GC diagnostic test, and the results (optimal cut-off values, sensitivities, specificities and AUC values) are depicted in Table 3. The four up-regulated metabolites including L-Carnitine, L-Proline, Pyruvaldehyde and PC(14:0/18:0) provided AUC values of 0.723 (sensitivity 57.1%, specificity 86.0%), 0.820 (sensitivity 71.4%, specificity 88.0%), 0.794 (sensitivity 100.0%, specificity 52.0%) and 0.769 (sensitivity 100.0%; specificity 50.0%) respectively, which implied a good distinctive ability in predicting intestinal-type GC. Another two down-regulated metabolites also have good independent predictive potential with AUC values from 0.780 to 0.849 (Table 3).

Table 3 ROC curve analysis of potential biomarkers in intestinal-type GC

No.	Groups	Metabolites	AUC	Sensitivity (%)	Specificity (%)
1	CSG-EGC	L-Carnitine	0.723	57.1%	86.0%
2	CSG-EGC	L-Proline	0.820	71.4%	88.0%
3	CSG-EGC	Pyruvaldehyde	0.794	100%	52.0%
4	CSG-EGC	PC(14:0/18:0)	0.769	100%	50.0%
5	CSG-EGC	LysoPC(14:0)	0.849	100%	62.0%
6	CSG-EGC	Lysinoalanine	0.780	100%	52.0%
7	CSG-EGC	Mixmodel 1	1	100%	100%
8	EGC-AGC	L-Proline	0.611	88.0%	42.9%
9	EGC-AGC	L-Valine	0.526	64.0%	57.1%
10	EGC-AGC	Adrenic acid	0.720	44.0%	100%
11	EGC-AGC	PC(O-18:0/0:0)	0.749	100%	57.1%
12	EGC-AGC	LysoPC(20:4(5Z,8Z,11Z,14Z))	0.731	76.0%	71.4%
13	EGC-AGC	Pyruvaldehyde	0.657	40.0%	100%
14	EGC-AGC	Mixmodel 2	0.931	76.0%	100%

Because the intestinal-type GC is a complex disease involving biochemical dysfunction in multiple pathways, a single biomarker could not be powerful to discriminate in clinical practice. Therefore, identifying a combination of biomarkers, which had greater predictive power, was particularly important. The 6 selected metabolites as the independent variables were combined together passed through binary logistic regression model with ROC curves to build the best biomarker panel. As a result, all six metabolites were used, which was termed as Mixmodel 1. The performance was calculated according to the equation (1) as follow.

$$\mathrm{Logit(P)}_{\mathrm{Mixmodel1}} = -1934.912 + 0.086 \times x_1 + 1.238 \times x_2 + 0.061 \times x_3 + 0.054 \times x_4 - 0.001 \times x_5 + 0.008 \times x_6 \quad (1)$$

where x_1, x_2, x_3, x_4, x_5 and x_6 are represent for the peak value of L-carnitine, L-proline, pyruvaldehyde, PC(14:0/18:0), LysoPC(14:0) and lysinoalanine, respectively.

$$P = \frac{e^{Logit(P)}}{1+e^{Logit(P)}} \quad (2)$$

The calculated results showed that the proposed biomarker panel model had AUC value of 1 (Fig. 3A), which meant that the multivariate model provided acceptable fit to the data across test samples.

Similarly, to confirm the diagnostic potential for the early detection of intestinal-type GC, we examined the AUC values in stage EGC to AGC patients. As listed in the table 4, 3 metabolites show good discrimination ability, with an AUC value above 0.7, along with 3 metabolites above 0.5. In addition, the biomarker panel was also applied to distinguish AGC patients with EGC patients, mining the potential ability for staging diagnosis. On the basis of binary logistic regression analysis, the plasma biomarker panel consisting of three metabolites, including L-proline, adrenic acid and PC(O-18:0/0:0), was defined as Mixmodel 2. The performance was calculated according to the following equation (3).

$$Logit(P)_{Mixmodel2} = 2.475 - 0.002 \times y_1 + 0.237 \times y_2 - 0.001 \times y_3 \quad (3)$$

where y1, y2 and y3 are represent for the peak value of L-Proline, Adrenic acid and PC(O-18:0/0:0), respectively. *Results show* that the biomarker panel had better diagnostic abilities than any single metabolite alone in distinguishing between intestinal-type EGC patients and AGC patients, with sensitivity, specificity, and AUC value of 0.931, 76.0%, and 100.0% at the best cut-off points (Fig. 3B, Table 3). As indicated by these results, the biomarker combinations presented herein serves not only to discriminate EGC from CSG patients, but is also capable of distinguishing stage I and II intestinal-type GC models with relatively high diagnostic accuracy.

Metabolic Pathway Analysis

On the basis of the detected differential metabolites, pathway analysis was performed by MetaboAnalyst 4.0 to uncover the global metabolic disorders in CSG and intestinal-type GC patients. Fig. 4A-B presents the major impacted pathways in the CSG-EGC and EGC-AGC groups, indicated by the red and orange colors (-log(p) >2 or impact value > 0.1). As shown in Fig. 3, the amino acid metabolism was discovered to be strikingly disturbed, including glycine, serine and threonine metabolism, valine, leucine and isoleucine biosynthesis and so on. The perturbations of central carbon metabolism (e.g., pyruvate metabolism) and lipid metabolism (e.g., glycerophospholipid metabolism, linoleic acid metabolism, alpha-linolenic acid metabolism and ether lipid metabolism) were also observed. The changes of detected differential metabolites related to the abnormal metabolic pathways, providing clues for underlying the potential metabolic mechanism in intestinal-type GC.

Discussion

In this study, high-throughput metabolomics couple with UPLC-Q-TOF/MS technology was utilized to investigate intestinal-type GC-related metabolic alterations and elucidate potential diagnostic biomarkers. The present evaluation was performed on patients with CSG and two subgroups of intestinal-type EGC and AGC subjects to search for the correlates between the small molecule metabolites and the disease progression. Most of the metabolites identified were altered on statistically significant level, derived mainly from general biochemical pathways related to amino acid metabolism, energy metabolism and lipid metabolism.

Amino acids, as the substrates for protein synthesis, are crucial for cancer cell migration and proliferation. Previous studies have associated amino acid metabolism aberrations with cancer development [13-14]. It is involved in multiple cancers that regulate several signaling pathways, including protein synthesis, cell growth, lipid biogenesis, autophagy and so on [15] In this study, L-proline was found to be up-regulated in intestinal-type EGC and AGC stage, and L-valine was also found significantly

up-regulated in AGC stage. High levels of proline could promote cell proliferation, energy production and resistance to oxidative stress (act as an antioxidant) [16-19]. L-valine is an essential and important functional amino acid involved in many growth and metabolic processes, and is also a glucogenic amino acid for biosynthesizing macromolecules (e.g., proteins and lipids), which are vital to the growth of cancer cell [20]. The accumulation of amino acids could ascribe to the proliferation by cancer cells, suggesting cancer transformation is linked with adaptive increases in protein synthesis [21].

Except a number of biologic functions, amino acid metabolism is also considered as an essential energy metabolism pathway of cancer cells to meet the high energy requirement [22]. For example, valine could be transformed into pyruvate for energy supply through aerobic glycolysis, resulting in the significant increase in pyruvate [23]. Thus, the up-regulated of valine in intestinal-type GC indicates that cancer cell energy metabolism may be significantly increased during cancer progression

Another important feature in intestinal-type GC progression was the apparent changes of lipids. It is well known that lipids play an important role at cellular and organismal levels, being the dominant structural components of biomembranes and energy storage entities [24]. Additionally, lipids participate in signal transduction and can be broken down into biologically active lipid mediators, which regulate some carcinogenic processes [25, 26]. In the present study, potential biomarkers analyses revealed significant alterations in plasma LysoPC and PC. The down-regulation of them may be mainly due to the increased demand for membrane constituents during malignant transformation, cancer invasion and metastasis. Dysregulation of choline phospholipid metabolism is associated with carcinogenesis and cancer progression, which has been verified in many biomarker studies [27-29], including studies of GC [30]. Thus, the abnormal levels of LysoPC and PC may be considered as important biomarkers for intestinal-type GC patients.

Glycolysis is a main metabolic mode of cancer cells. Most cancer cells mainly use aerobic glycolysis to generate energy rather than mitochondrial oxidative phosphorylation and produce great numbers of lactate and acidic metabolites, which is known as the “Warburg effect” [31]. Methylglyoxal (also called pyruvaldehyde) is a cytotoxic reactive intermediate of glycolysis [32], whose overexpression was observed in a variety of human cancers [33, 34]. The main metabolic pathway leading to methylglyoxal is related to carbohydrate metabolism and involves enzymatic and nonenzymatic degradation of the triose-phosphate intermediates dihydroxyacetone phosphate and glyceraldehyde 3-phosphate deriving from glycolysis. It should be noted that methylglyoxal can react rapidly with DNA and proteins to produce advanced-glycated end products, and thus promote cell death [35].

A comprehensive understanding of metabolic alterations associated with cancer stages would be helpful in the development of intestinal-type GC. Among the all differential metabolites, there were some metabolites that showed a good potential to differentiate with AUC values more than 0.8, such as L-proline, LysoPC(14:0) (Table 4). However, a question arises as to whether one molecule has sufficient potential in intestinal-type GC detection. Based on the results of previous cancer biomarker studies, it can be assumed that the most efficient sample discrimination will be obtained using metabolite panels. Therefore, we built logistic regression models consisting of multiple metabolites. The AUC values (> 0.931) of multivariate ROC curve were higher than that obtained for single metabolite (Table 3) and the metabolite panels model turned out to be sensitivity enough to distinguish patients correctly. Therefore, the application of a combination strategy allows for better early diagnosis of intestinal-type GC and precancerous stages.

In summary, this study suggests that the biomarker panels possessed the potential value for the diagnosis of intestinal-type GC stages. The identified potential biomarkers and biological pathways might provide new directions for further studies in cancer growth and development. However, the strict inclusion and exclusion criteria decreased the number of recruited patients, and further research should involve the inclusion of multicenter subjects with intestinal-type GC of different stages, to better evaluate the accuracy of the developed models in early diagnosis.

Conclusion

In this study, UPLC-Q-TOF/MS plasma metabolomics has been successfully applied for biomarker screening in intestinal-type GC. Based on differential metabolites signatures, biomarker panels were defined for the diagnosis of EGC with satisfactory

discrimination performance, as well as for AGC (AUC > 0.931). Metabolic pathway analysis indicated that changes in most potential plasma biomarkers were correlated with general biochemical pathways (amino acid metabolism and lipid metabolism), implying enhanced energy production and cell proliferation. The study highlights the potential advantages of biomarker panels in real clinical diagnostics, which can be used as a promising tool for early-stage intestinal-type GC diagnosis and prognosis.

Abbreviations

AGC: Advanced gastric cancer; AUC: area under the curve; CSG: Chronic superficial gastritis; EGC: Early gastric cancer; GC: Gastric cancer; LysoPC: lysophosphatidylcholines; OPLS-DA: Orthogonal partial least squares-discriminant analysis; PC: phosphatidylcholines; PCA: Principal components analysis; QC: Quality control; ROC: Receiver operating characteristic curve; UPLC-Q-TOF/MS: Ultra-high performance liquid chromatography coupled with quadrupole-time-of-flight mass spectrometry; VIP: Variable importance in projection.

Declarations

Acknowledgements

Not applicable.

Ethnical approval and consent to participate

According to the Declaration of Helsinki, this study project was evaluated and approved by Institutional Review Board of the 903rd Hospital of PLA (20140501; Hangzhou, China) and Institutional Review Board of People's Hospital of Yangzhong City (IRB201404; Yangzhong, China). Written informed consent was obtained from all participants.

Authors' contributions

SK Y and XW conceived and designed the study. XW, SS L, J L, JM M and ZL H collected the clinical data and performed the experiments. LJ D drafted the first version of the manuscript. SK Y, XX and HZ J revised the manuscript toghther. All authors contributed to the interpretation of the results, edited and approved the final manuscript.

Funding

This work was supported by the Hangzhou Science and Technology Commission (20140633B41) and the Medical Innovation Project of PLA Nanjing Military Area Command (2013MS150). The Committee of Hangzhou Science and Technology Commission and Medical Innovation Project of PLA Nanjing Military Area Command made a detailed discussion of the scientific validity, reasonableness and feasibility of this study and finally decided to support this study.

Availability of data and materials

All the necessary materials can be found in the text or supplementary materials. Due to the privacy policy, the confidential data materials could only be obtained with the permission of the corresponding authors.

Consent for publication

Not applicable.

Competing interests

The authors declare that they have no conflict of interests.

References

1. Bray F, Ferlay J, Soerjomataram I, et al. Global cancer statistics 2018: GLOBOCAN estimates of incidence and mortality worldwide for 36 cancers in 185 countries. CA Cancer J Clin. 2018; 68(6): 394-424.
2. D'Angelica M, Gonen M, Brennan MF, et al. Patterns of initial recurrence in completely resected gastric adenocarcinoma. Ann Surg. 2004; 240: 808–16.
3. Kamangar F, Dores GM, Anderson WF. Patterns of cancer incidence, mortality, and prevalence across five continents: defining priorities to reduce cancer disparities in different geographic regions of the world. J Clin Oncol. 2006; 24: 2137–50.
4. Correa P. A human model of gastric carcinogenesis. Cancer Res. 1988; 48: 3554– 60.
5. Naresh Doni Jayavelu, Nadav S Bar. Metabolomic studies of human gastric cancer: Review. World J Gastroenterol, 2014, 20(25): 8092-8101.
6. Weiss RH, Kim K. Metabolomics in the study of kidney diseases. Nat Rev Nephrol. 2011; 8: 22-33.
7. Wang Z, Liu XY, Liu X, et al. UPLC-MS based urine untargeted metabolomic analyses to differentiate bladder cancer from renal cell carcinoma. BMC Cancer. 2019; 19: 1195.
8. Dettmer K, Aronov PA, Hammock BD. Mass spectrometry-based metabolomics. Mass Spectrom Rev. 2007; 26: 51-78.
9. Tang YQ, Li Z, Lazar L, et al. Metabolomics workflow for lung cancer: Discovery of biomarkers. Clin Chim ACTA. 2019; 495: 436-45.
10. Sarma SN, Kimpe LE, Doyon VC. A metabolomics study on effects of polyaromatic compounds in oil sand extracts on the respiratory, hepatic and nervous systems using three human cell lines. Environ Res. 2019; 178: 108680.
11. Costello E. A metabolomics-based biomarker signature discriminates pancreatic cancer from chronic pancreatitis. Gut. 2018; 67(1): 2-3.
12. Zheng XZ, Mao XH, Xu K, et al. Massive Endoscopic Screening for Esophageal and Gastric Cancers in a High-Risk Area of China. PLoS One. 2015; 10(12): e0145097.
13. Christensen HN. Role of amino acid transport and countertransport in nutrition and metabolism. Physiol Rev. 1990; 70: 43-77.
14. Lai HS, Lee JC, Lee PH, et al. Plasma free amino acid profile in cancer patients. Semin Cancer Biol. 2005; 15: 267-76.
15. O'Connell TM. The complex role of branched chain amino acids in diabetes and cancer. Metabolites. 2013; 3 (4): 931-45.
16. Liu W, Hancock CN, Fischer JW, et al. Proline biosynthesis augments tumor cell growth and aerobic glycolysis: involvement of pyridine nucleotides. Sci Rep-UK. 2015; 5: 17206.
17. Elia I, Broekaert D, Christen S, et al. Proline metabolism supports metastasis formation and could be inhibited to selectively target metastasizing cancer cells. Nat Commun. 2017; 8: 15267.
18. Sahu N. Cruz DD, Gao M, et al. Proline starvation induces unresolved ER stress and hinders mTORC1-dependent tumorigenesis. Cell Metab. 2016; 24: 753-61.
19. Szabados L, Savouré Arnould. Proline: a multifunctional amino acid. Trends Plant Sci. 2010; 15: 89-97.
20. Phang JM. Proline Metabolism in Cell Regulation and Cancer Biology: Recent Advances and Hypotheses. Antioxid Redox Sign. 2019; 30(4): 635–49.
21. Eley HL, Russell ST, Tisdale MJ. Effect of branched-chain amino acids on muscle atrophy in cancer cachexia. Biochem J. 2007; 407(1): 113–20.
22. Hong Y, Ho KS, Eu KW, et al. A susceptibility gene set for early onset colorectal cancer that integrates diverse signaling pathways: implication for tumorigenesis. Clin Cancer Res. 2007; 13: 1107–14.
23. Dang CV. Links between metabolism and cancer. Genes Dev. 2012; 26: 877–90.
24. Chaneton B, Hillmann P, Zheng L, et al. Serine is a natural ligand and allosteric activator of pyruvate kinase M2. Nature. 2012; 491: 458–62.
25. Santos CR, Schulze A. Lipid metabolism in cancer. FEBS J. 2012; 279: 2610–23.
26. Perrotti F, Rosa C, Cicalini I, et al. Advances in lipidomics for cancer biomarkers discovery. Int J Mol Sci. 2016; 17: 1992.

27. Klupczynska A, Plewa S, Kasprzyk M, et al. Serum lipidome screening in patients with stage I non-small cell lung cancer. Clin Exp Med. 2019; 19(4): 505–13.
28. Lu YH, Huang C, Gao L, et al. Identification of serum biomarkers associated with hepatitis B virus-related hepatocellular carcinoma and liver cirrhosis using mass-spectrometry-based metabolomics. Metabolomics. 2015; 11: 1526–38.
29. Li JN, Xie HY, Li A, et al. Distinct plasma lipids profiles of recurrent ovarian cancer by liquid chromatography-mass spectrometry. Oncotarget, 2017; 8(29): 46834-45.
30. Cheng ML, Bhujwalla ZM and Glunde K. Targeting Phospholipid Metabolism in Cancer. Front Oncol. 2016; 6: 266.
31. Warburg O. On the origin of cancer cells. Science. 1956; 123: 309-314.
32. Kalapos MP. Methylglyoxal in living organisms: chemistry, biochemistry, toxicology and biological implications. Toxicol. Lett. 1999; 110: 145–175.
33. Baunacke M, Horn LC, Trettner S, et al. Exploring glyoxalasel expression in prostate cancer tissues: targeting the enzyme by ethyl pyruvate defangs some malignancy-associated properties. Prostat. 2014; 74 (1): 48-60.
34. Fonseca-Sánchez MA, Rodríguez-Cuevas S, Mendoza-Hernández G, et al. Breast cancer proteomics reveals a positive correlation between glyoxalase 1 expression and high tumor grade. Int J Oncol. 2012; 41: 670-680.
35. Desai K, Wu L. Methylglyoxal and advanced glycation endproducts: New therapeutic horizons? Recent Pat. Cardiovasc. Drug Discov. 2007; 2: 89-99.

Figures

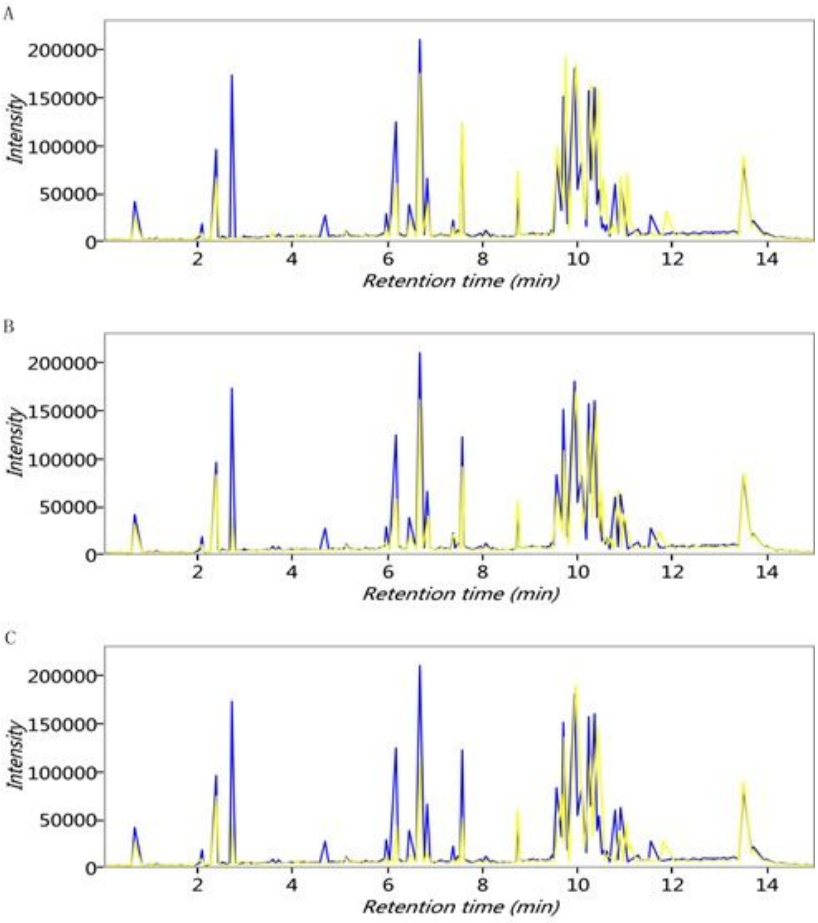

Figure 1

Typical total ion current chromatograms of diseases (color-blue) and QC samples (color-yellow) in positive mode UPLC-Q-TOF/MS analyses. (A) CSG; (B) EGC; (C) AGC.

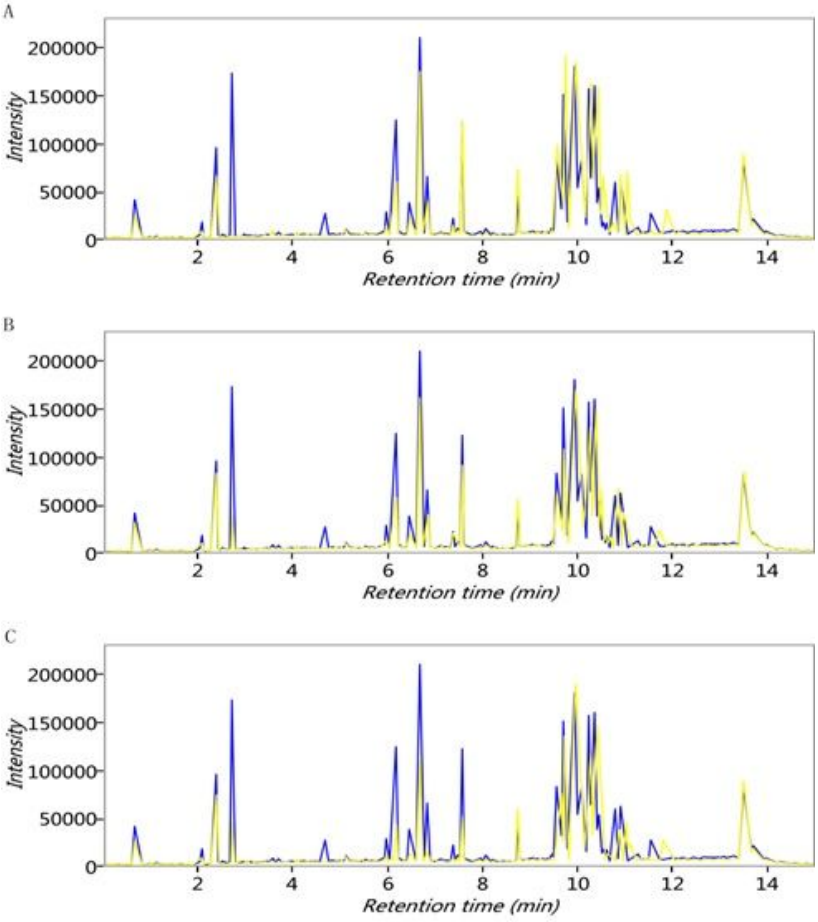

Figure 1

Typical total ion current chromatograms of diseases (color-blue) and QC samples (color-yellow) in positive mode UPLC-Q-TOF/MS analyses. (A) CSG; (B) EGC; (C) AGC.

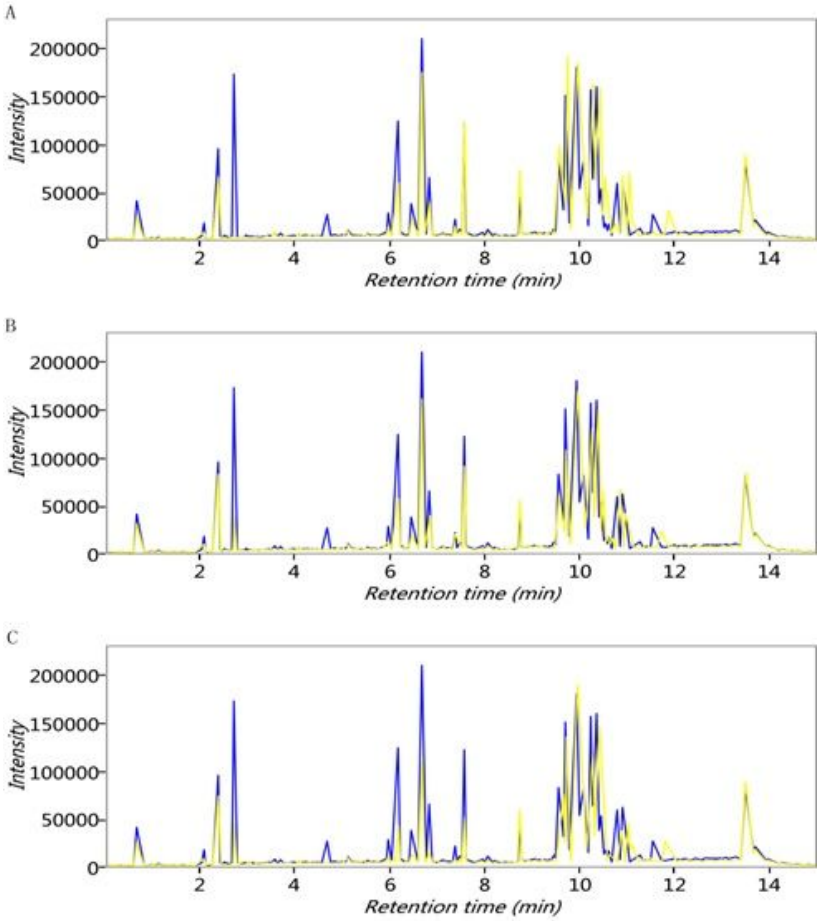

Figure 1

Typical total ion current chromatograms of diseases (color-blue) and QC samples (color-yellow) in positive mode UPLC-Q-TOF/MS analyses. (A) CSG; (B) EGC; (C) AGC.

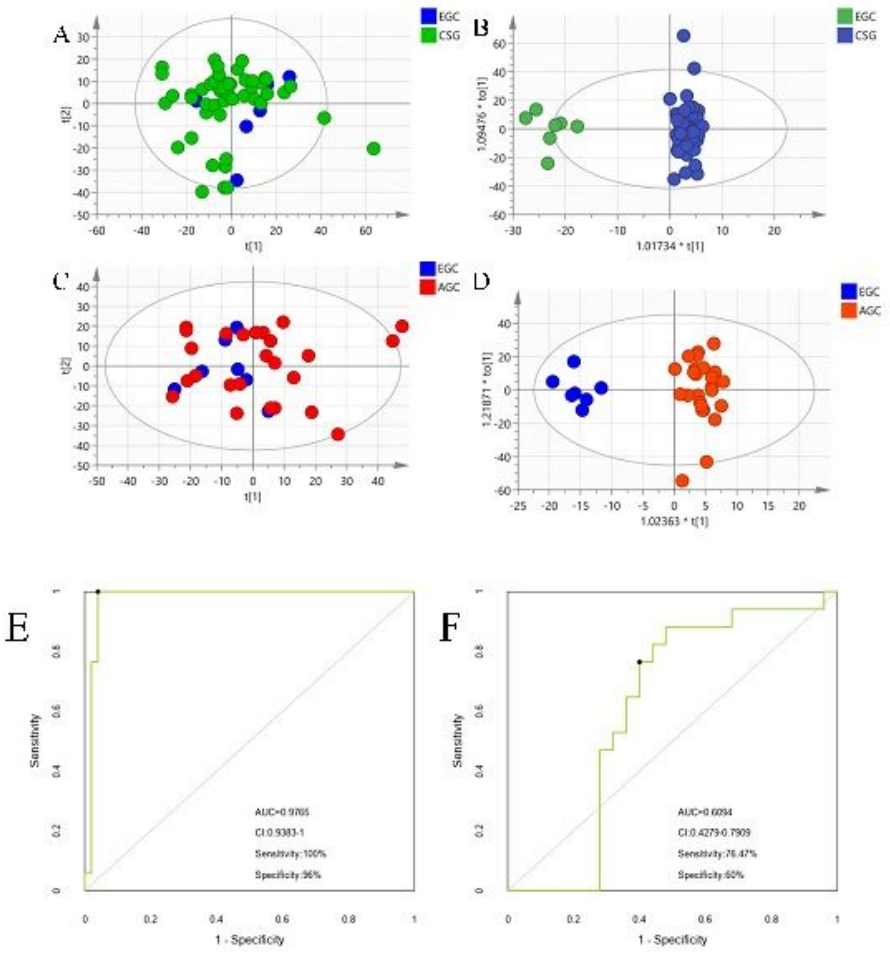

Figure 2

Multivariate statistical analyses to distinguish the metabolic phenotypes between different groups. (A) PCA score plot of targeted metabolites collected from CSG (light blue) and EGC (green) groups; (B) OPLS-DA score plot of targeted metabolites collected from CSG (light blue) and EGC (green) groups; (C) PCA score plot of targeted metabolites collected from EGC (blue) and AGC (red) groups; (D) OPLS-DA score plot of targeted metabolites collected from EGC (blue) and AGC (red) groups; (E) ROC curve of the Random Forest classifiers between CSG and EGC groups; (F) ROC curve of the Random Forest classifiers between EGC and AGC groups.

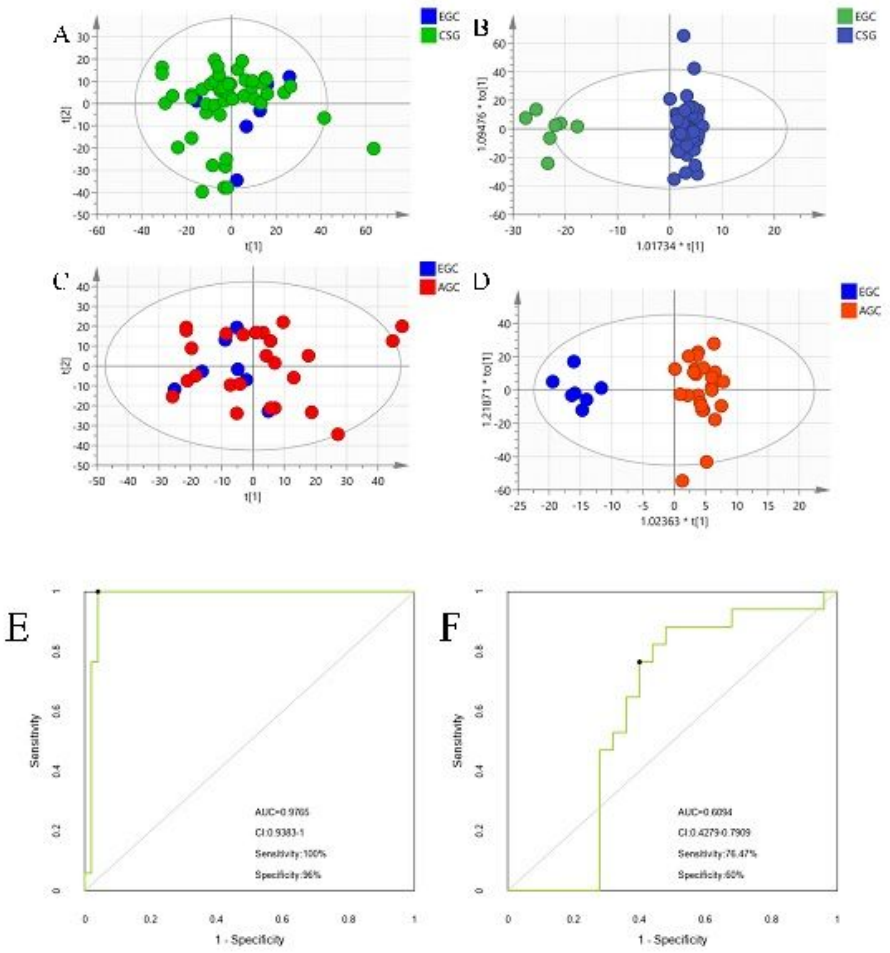

Figure 2

Multivariate statistical analyses to distinguish the metabolic phenotypes between different groups. (A) PCA score plot of targeted metabolites collected from CSG (light blue) and EGC (green) groups; (B) OPLS-DA score plot of targeted metabolites collected from CSG (light blue) and EGC (green) groups; (C) PCA score plot of targeted metabolites collected from EGC (blue) and AGC (red) groups; (D) OPLS-DA score plot of targeted metabolites collected from EGC (blue) and AGC (red) groups; (E) ROC curve of the Random Forest classifiers between CSG and EGC groups; (F) ROC curve of the Random Forest classifiers between EGC and AGC groups.

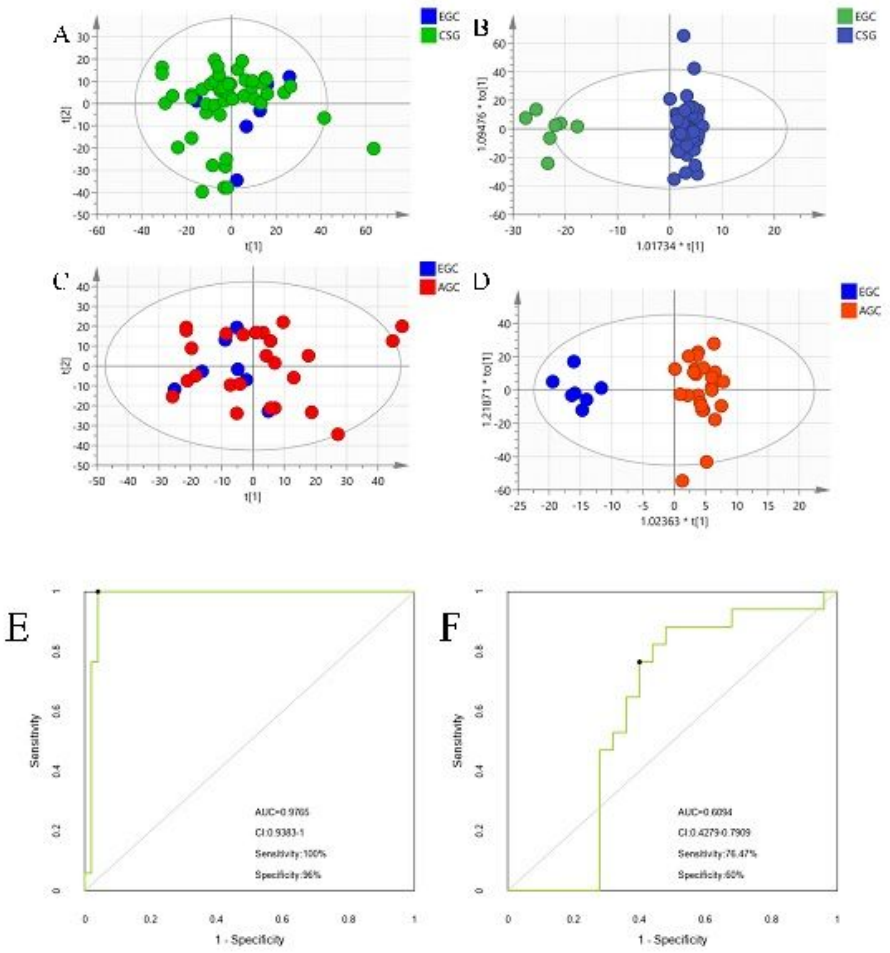

Figure 2

Multivariate statistical analyses to distinguish the metabolic phenotypes between different groups. (A) PCA score plot of targeted metabolites collected from CSG (light blue) and EGC (green) groups; (B) OPLS-DA score plot of targeted metabolites collected from CSG (light blue) and EGC (green) groups; (C) PCA score plot of targeted metabolites collected from EGC (blue) and AGC (red) groups; (D) OPLS-DA score plot of targeted metabolites collected from EGC (blue) and AGC (red) groups; (E) ROC curve of the Random Forest classifiers between CSG and EGC groups; (F) ROC curve of the Random Forest classifiers between EGC and AGC groups.

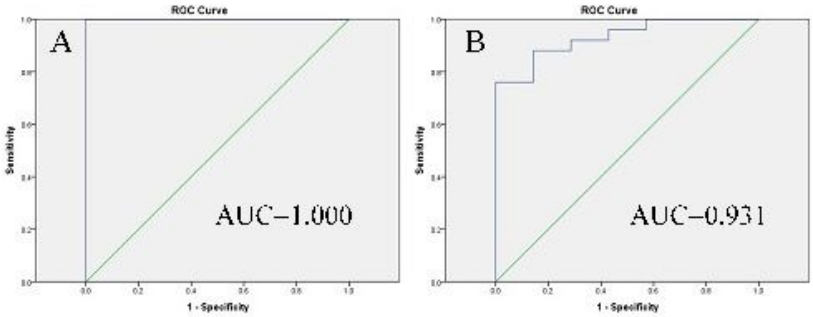

Figure 3

ROC curves based on binary logistic regression model with biomarkers combination. (A) Mixmodel 1. (B) Mixmodel 2.

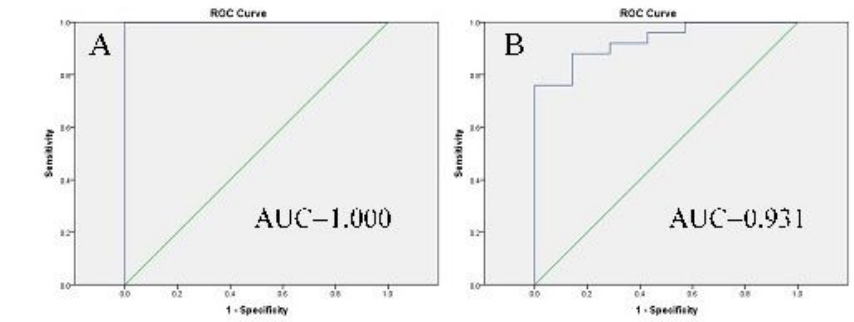

Figure 3

ROC curves based on binary logistic regression model with biomarkers combination. (A) Mixmodel 1. (B) Mixmodel 2.

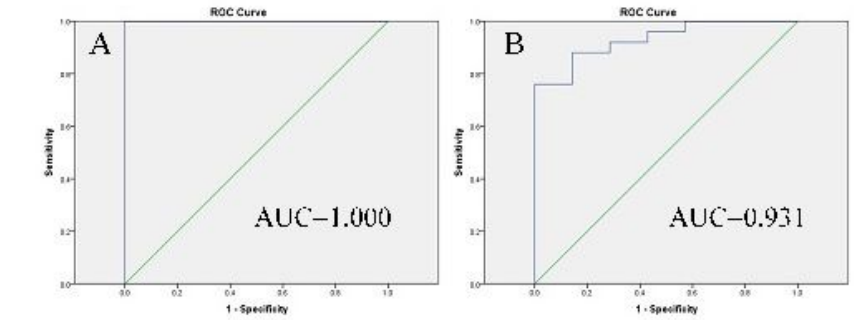

Figure 3

ROC curves based on binary logistic regression model with biomarkers combination. (A) Mixmodel 1. (B) Mixmodel 2.

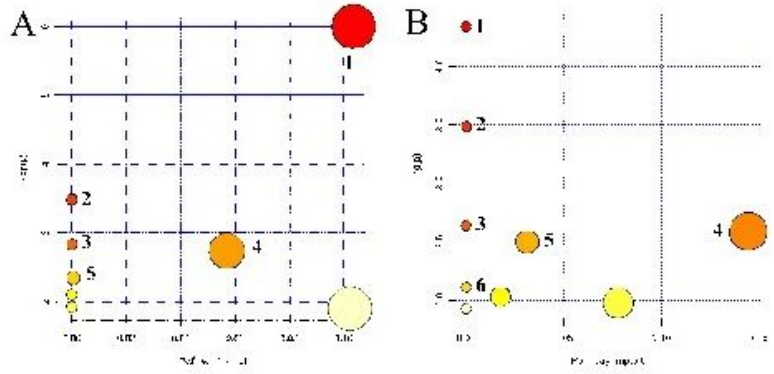

Figure 4

Metabolic pathway analysis in intestinal-type GC. (A) CSG and EGC. 1) Glycerophospholipid metabolism; 2) Linoleic acid metabolism; 3) alpha-Linolenic acid metabolism; 4) Pyruvate metabolism; 5) Glycine, serine and threonine metabolism. (B) EGC and AGC. 1) Aminoacyl-tRNA biosynthesis; 2) Valine, leucine and isoleucine biosynthesis; 3) Pantothenate and CoA biosynthesis; 4) Ether lipid metabolism; 5) Pyruvate metabolism; 6) Glycine, serine and threonine metabolism.

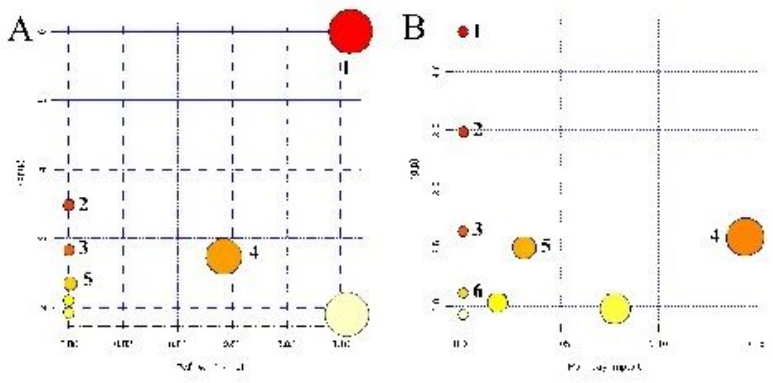

Figure 4

Metabolic pathway analysis in intestinal-type GC. (A) CSG and EGC. 1) Glycerophospholipid metabolism; 2) Linoleic acid metabolism; 3) alpha-Linolenic acid metabolism; 4) Pyruvate metabolism; 5) Glycine, serine and threonine metabolism. (B) EGC and AGC. 1) Aminoacyl-tRNA biosynthesis; 2) Valine, leucine and isoleucine biosynthesis; 3) Pantothenate and CoA biosynthesis; 4) Ether lipid metabolism; 5) Pyruvate metabolism; 6) Glycine, serine and threonine metabolism.

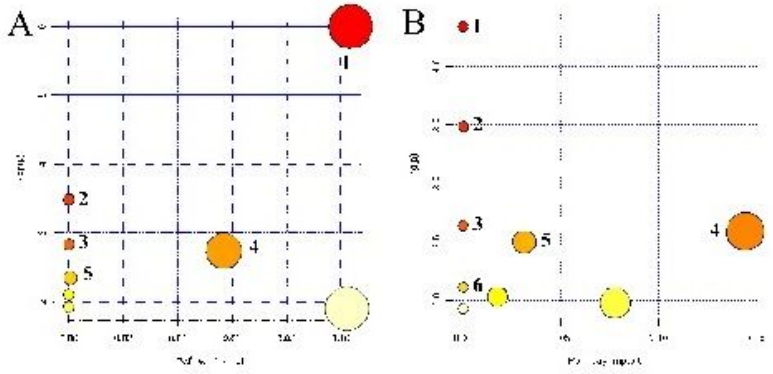

Figure 4

Metabolic pathway analysis in intestinal-type GC. (A) CSG and EGC. 1) Glycerophospholipid metabolism; 2) Linoleic acid metabolism; 3) alpha-Linolenic acid metabolism; 4) Pyruvate metabolism; 5) Glycine, serine and threonine metabolism. (B) EGC and AGC. 1) Aminoacyl-tRNA biosynthesis; 2) Valine, leucine and isoleucine biosynthesis; 3) Pantothenate and CoA biosynthesis; 4) Ether lipid metabolism; 5) Pyruvate metabolism; 6) Glycine, serine and threonine metabolism.

Supplementary Files

This is a list of supplementary files associated with this preprint. Click to download.

- Supplymentarymaterials.pdf
- Supplymentarymaterials.pdf
- Supplymentarymaterials.pdf
- Supplymentarymaterialsrowdata.xlsx
- Supplymentarymaterialsrowdata.xlsx
- Supplymentarymaterialsrowdata.xlsx